This project has received funding from the European Union's Horizon 2020 Research and Innovation programme under Grant Agreement No 730871.

Magnetic field penetration method for developing superconducting thin films for SRF

Daniel Turner
Lancaster University
Daresbury Laboratory

The 5th ARIES Annual Meeting, 03-02 May 2022

SRF limitations

- SRF cavities have a large Q_0 (10^{10}) and are more efficient than normal conducting cavities for continuous wave applications.
- Currently the material used in SRF cavities is bulk Nb.
  - Element with the largest Tc.
  - Critical fields (approx.) :
    - B_{c1} =170 mT
    - B_{c2} =240 mT ≈ B_{sh} – The superheating field.
  - Imperfections on the surface cause localised heating due to the B field, and therefore local quenches.
  - Theoretical accelerating gradient limit is 57 MV/m.
  - Starting to reach the limits of Nb cavities ~ 40 MV/m.
- Increasing E_{acc} allows smaller accelerators to be built, therefore saving money on infrastructure.

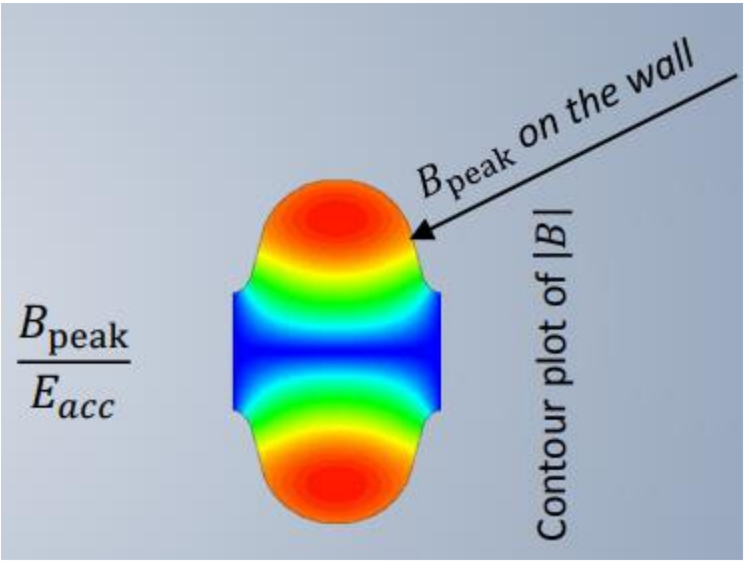

Erk JENSEN, RF Basics and TM Cavities, SRF 2019 Tutorials

Increasing SRF accelerating gradient (E_{acc})

- Gurevich proposed to use the multilayer structures to increase E_{acc}:
  - Superconducting-Superconducting bi layer – Consists of a 'dirty' SC layer with a larger λ_L, followed by SC bulk with smaller λ_L.
  - Superconducting Insulating Superconducting structure – SC layers separated by a dielectric/insulating layer.

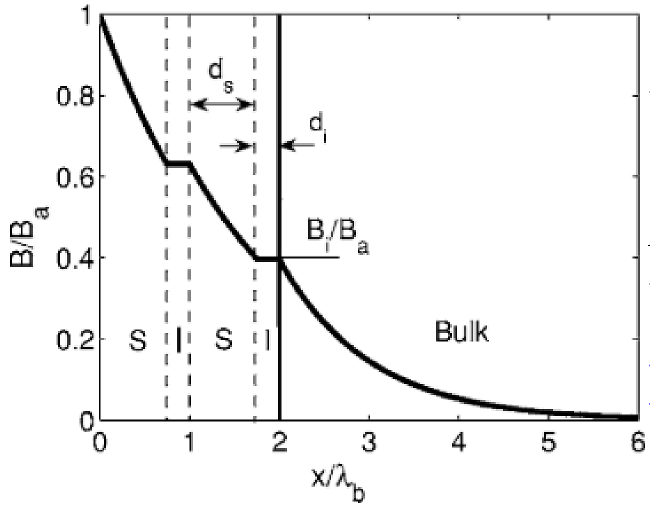

Gurevich, A. (2006). Enhancement of rf breakdown field of superconductors by multilayer coating. Applied Physics Letters, 88(1), 012511. https://doi.org/10.1063/1.2162264

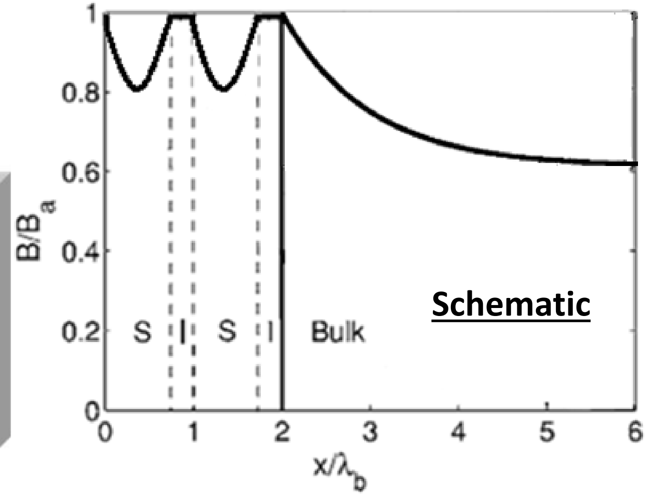

Schematic of a SIS multilayer in a VSM setup.

Kubo, T. (2017). Multilayer coating for higher accelerating fields in superconducting radio-frequency cavities: a review of theoretical aspects. In Superconductor Science and Technology (Vol. 30, Issue 2). https://doi.org/10.1088/1361-6668/30/2/023001

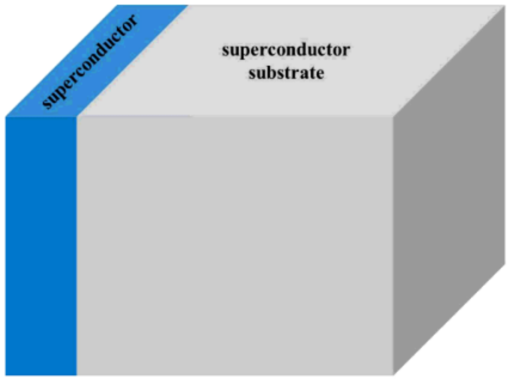

Bi-Layer

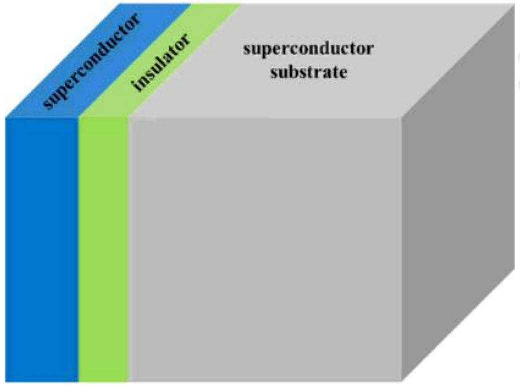

SIS Structure

Increasing SRF accelerating gradient (E_{acc})

- Gurevich proposed to use the multilayer structures to increa
  - Su
    Co
    fol
  - Su
    stru
    dielectric/insulating layer.

But first – These structures need to be tested:

- Depositing small samples is faster, easier and cheaper than cavities.
- Flat samples are easier to deposit than 3D structures.
- DC can provide insight into critical fields of superconductors.
- Allows coating parameter optimization, and insight for materials that are potentially useful for SRF applications.

What do we want from a local magnetometer:

- To imitate cavity operation – Magnetic field applied from one side of the sample.
- Applied field much smaller than the sample to eliminate edge effects.

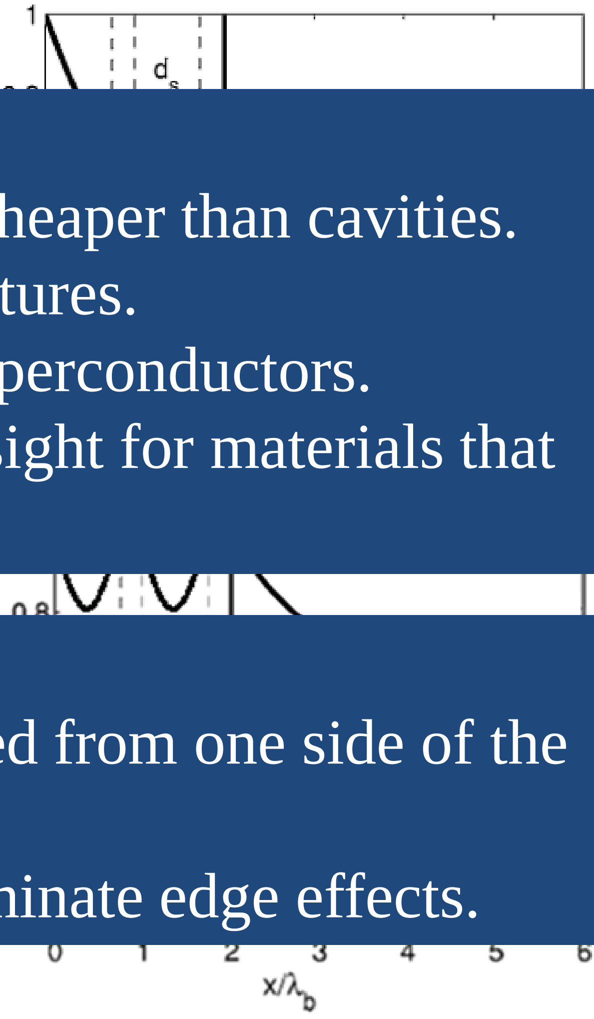

Gurevich, A. (2006). Enhancement of rf akdown field of erconductors by ltilayer coating. plied Physics ters, 88(1), 2511. os://doi.org/10.10 1.2162264

Schematic of SIS nultilayer in VSM setup.

Kubo, T. (2017). M for higher acceler superconducting r cavities: a review aspects. In Superconductor Science and Technology (Vol. 30, Issue 2). https://doi.org/10.1088/1361-6668/30/2/023001

Bi-Layer SIS Structure

Field penetration concept

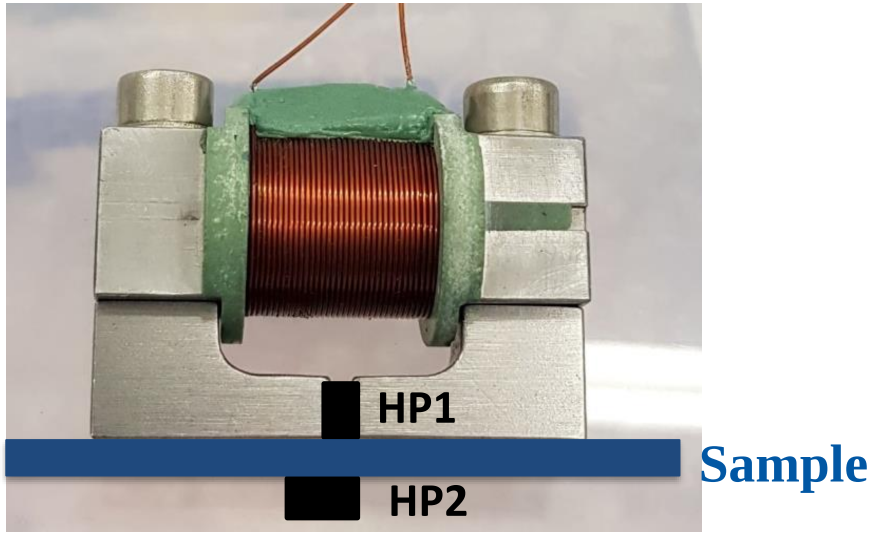

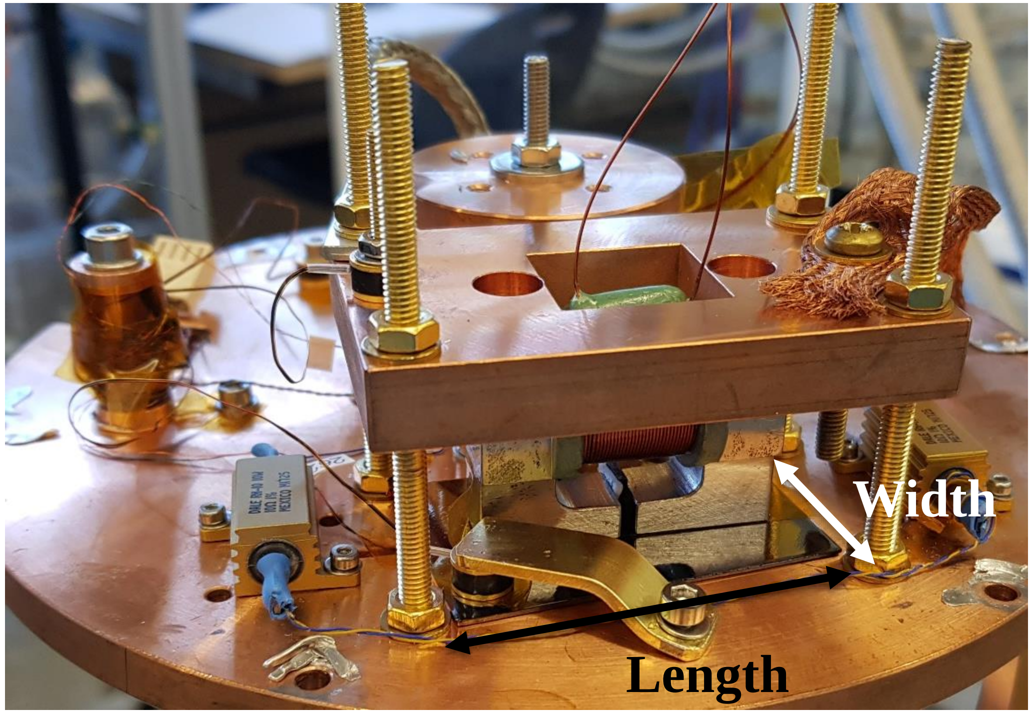

- DC magnetic field parallel to the surface.
- Field local to the sample surface:
  - Avoid edge effect.
  - Allow possibility if sample scanning.
- Magnetic field applied from one side of the sample to the opposing side, similar to an SRF cavity.
- Applied and penetrated field measured by Hall probe sensors.

Cryogenic facility

Thermal radiation shields

Stage 2 – Sample testing stage, T≈2.6 K

LTS to HTS join

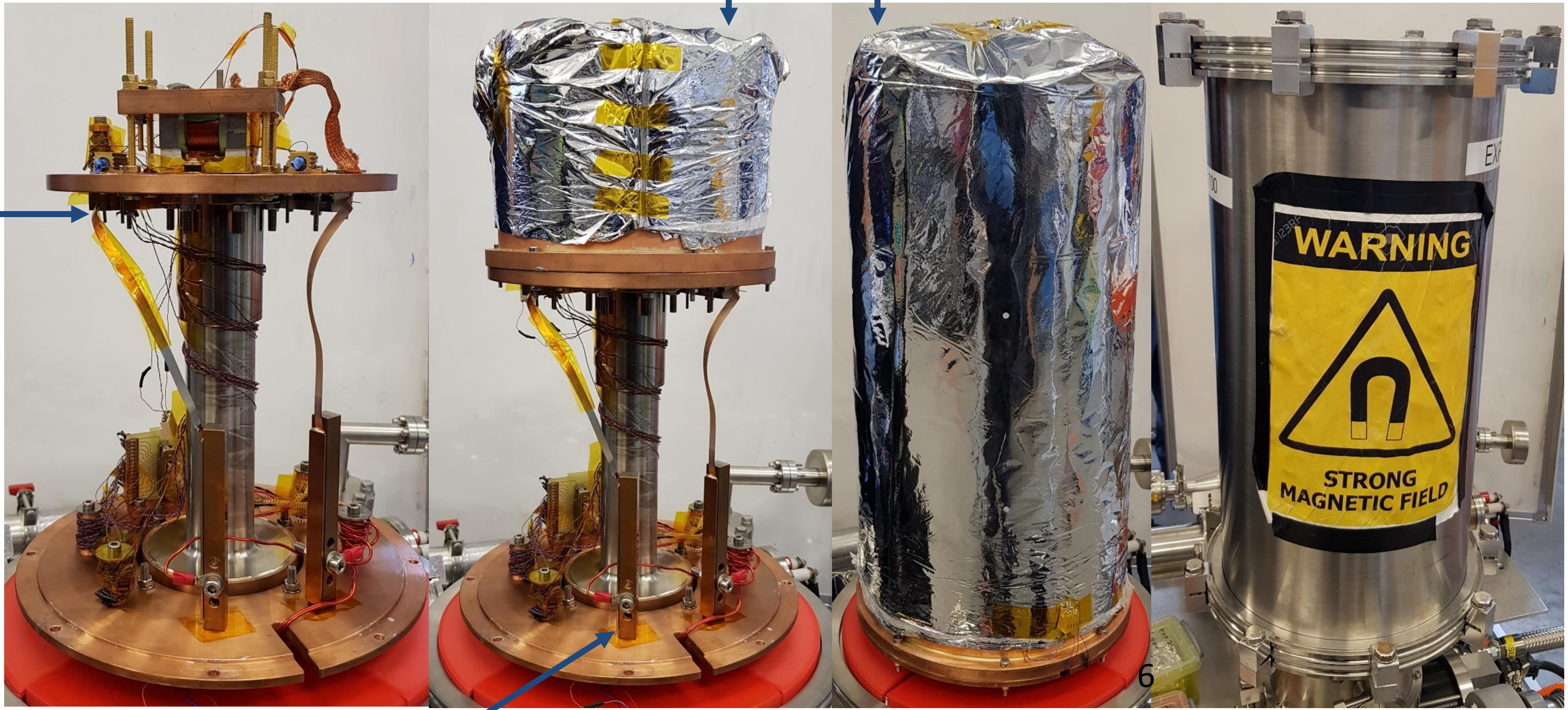

Stage 1 – Thermalisation of wires, heat sink for heat shields, and normal conducting to HTS join

Type I results - Pb

Method:

- Zero field cool-down from above T_c (≈7.2 K).
- Increase the applied magnetic field (B_1).
- Small increase in Hall probe sensor 2 (B_2) indicating B leaking around the sample, indicated by line B_1K_2.
- Sharp increase in B_2, indicates the field of full flux penetration (B_{fp}).
- After B_{fp}, the area the magnetic field has penetrated becomes normal conducting, such that $B_2(B_1)$ lies on B_1K_1.
- Magnet is degaussed, the sample is heated above T_c, and the test is repeated at the next set T.

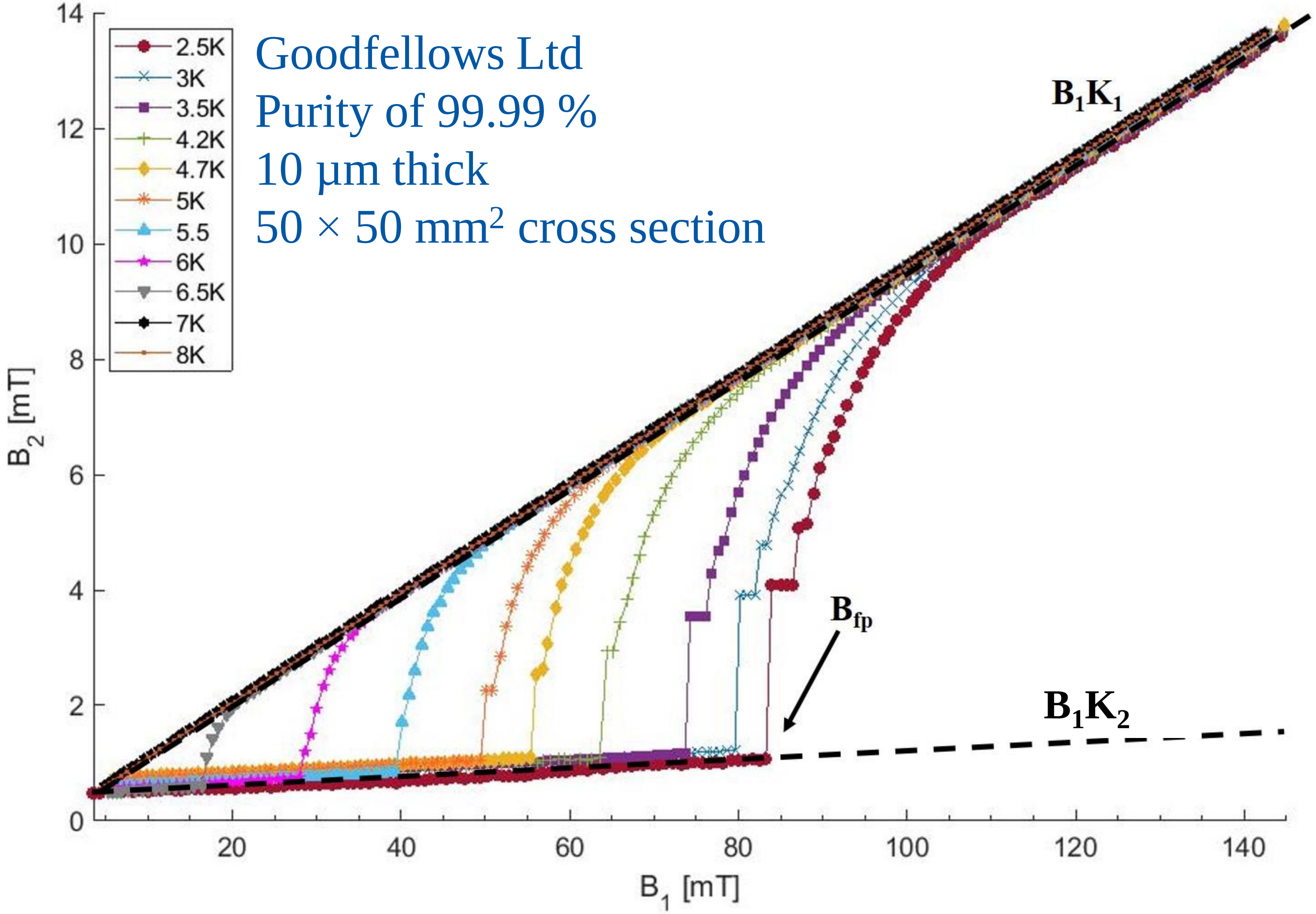

Note: B_{fp} is the field at which the applied field has broken through the sample, and **not** B_{c1}.

The effect of geometry

Multiple Pb sample sizes tested at 3.5 K

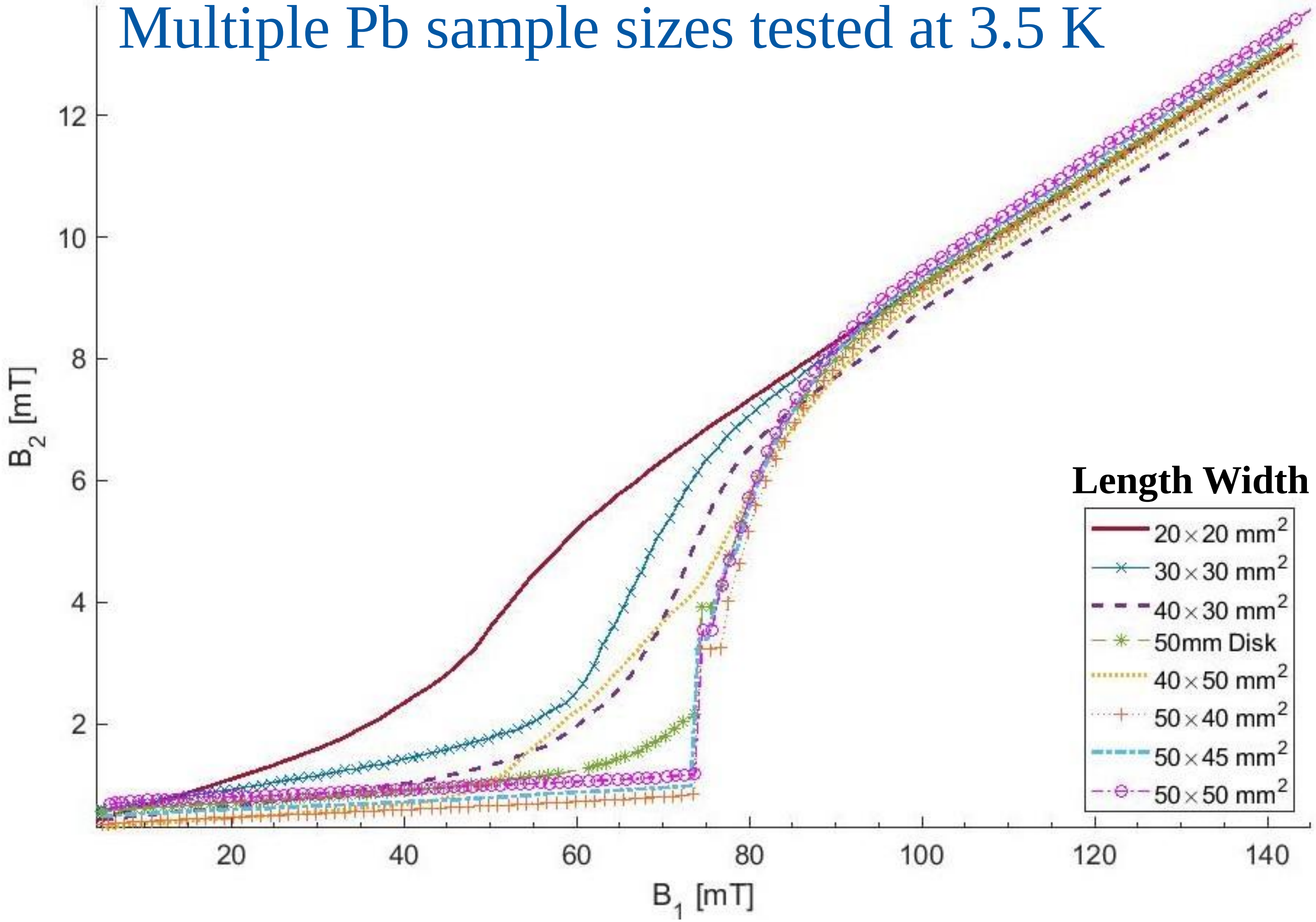

- Starting with a sample size of 50 × 50 mm², the sample was slowly reduced.
- Comparing the raw data (left) it can be seen that reducing the sample size increases B_1K_2.
- Reducing the sample 'length' has a greater affect on B_1K_2 than the width.
- B_1K_2 is not always linear, which can skew B_{fp} results using the normalisation method.
- It is still possible to extract B_{fp}.

Finding B_{fp}

Second derivative method

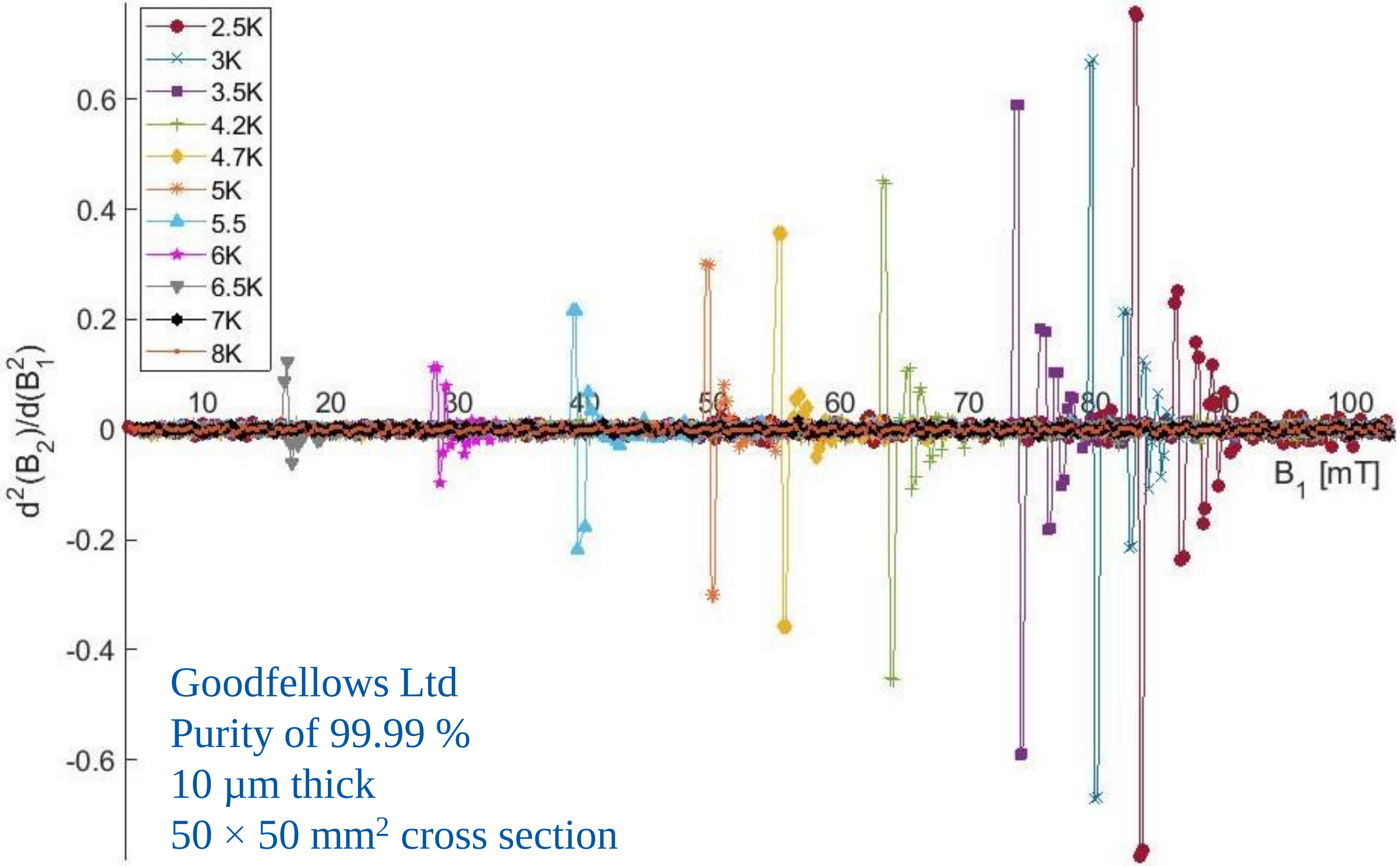

Goodfellows Ltd
Purity of 99.99 %
10 µm thick
50 × 50 mm^2 cross section

- The rate of change of B_2 is plotted against B_1.

$$\frac{d^2(B_2)}{d(B_1)^2}$$

- The greatest change is defined as B_{fp}.
- Smaller peaks represent smaller jumps – likely the normal conducting area of the sample increasing, allowing more magnetic field through.
- Noisy data is smoothed using robust linear regression.

B_{fp} as a function of T^2

B_{fp} taken using the second derivative method

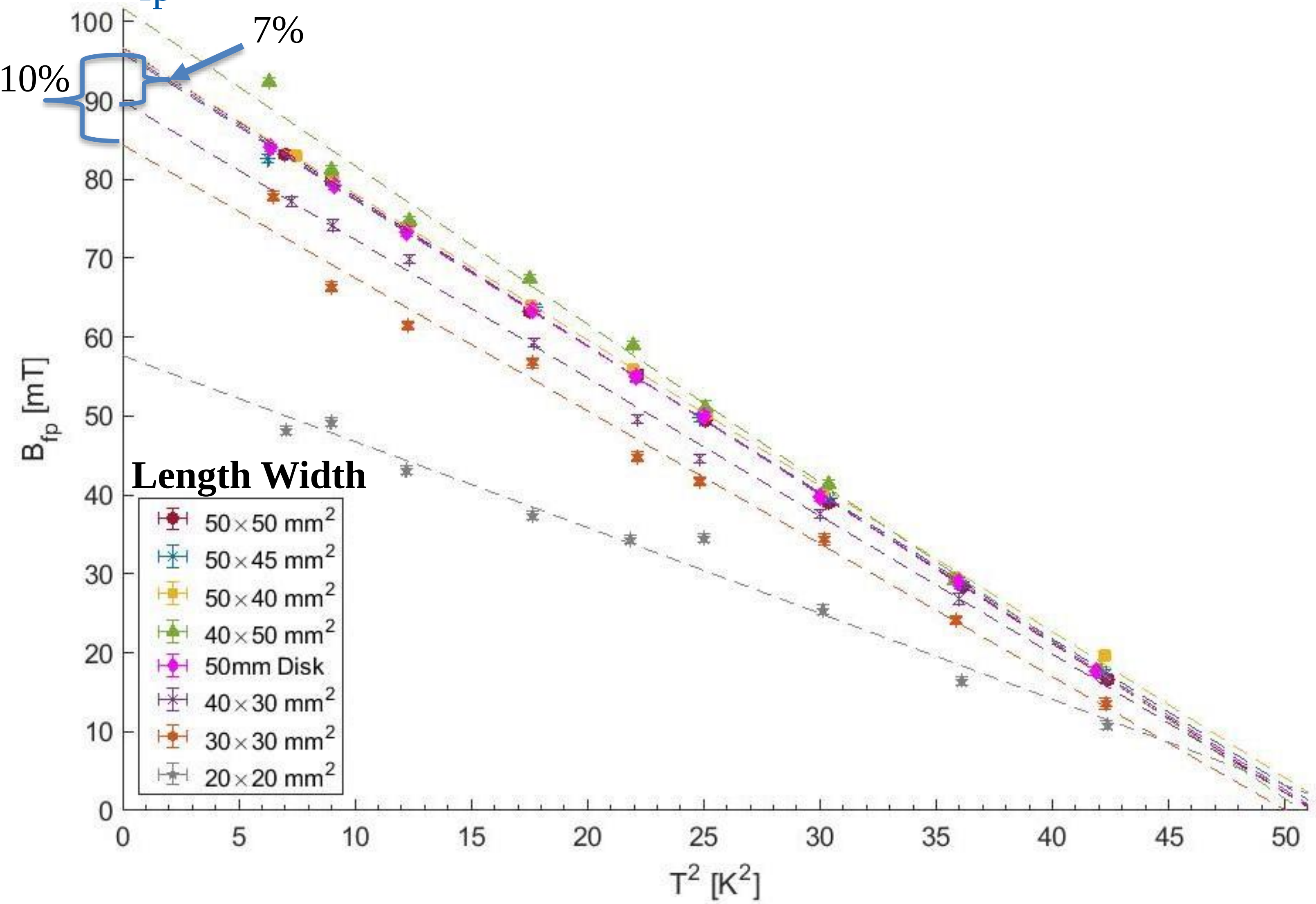

- B_{fp} as a function of T^2 has a linear trend.
- B_{fp}(0 K) and T_c(0 mT) can be extracted from this graph.
- 7% decrease in B_{fp} when the sample size is reduced to 40×30 mm² (from 50×50 mm²).
- 10% decrease in B_{fp} when the sample size is reduced to 30×30 mm² (from 50×50 mm²).
- Therefore sample size should be kept as large as possible to ensure reliable results.

Type II results - Nb

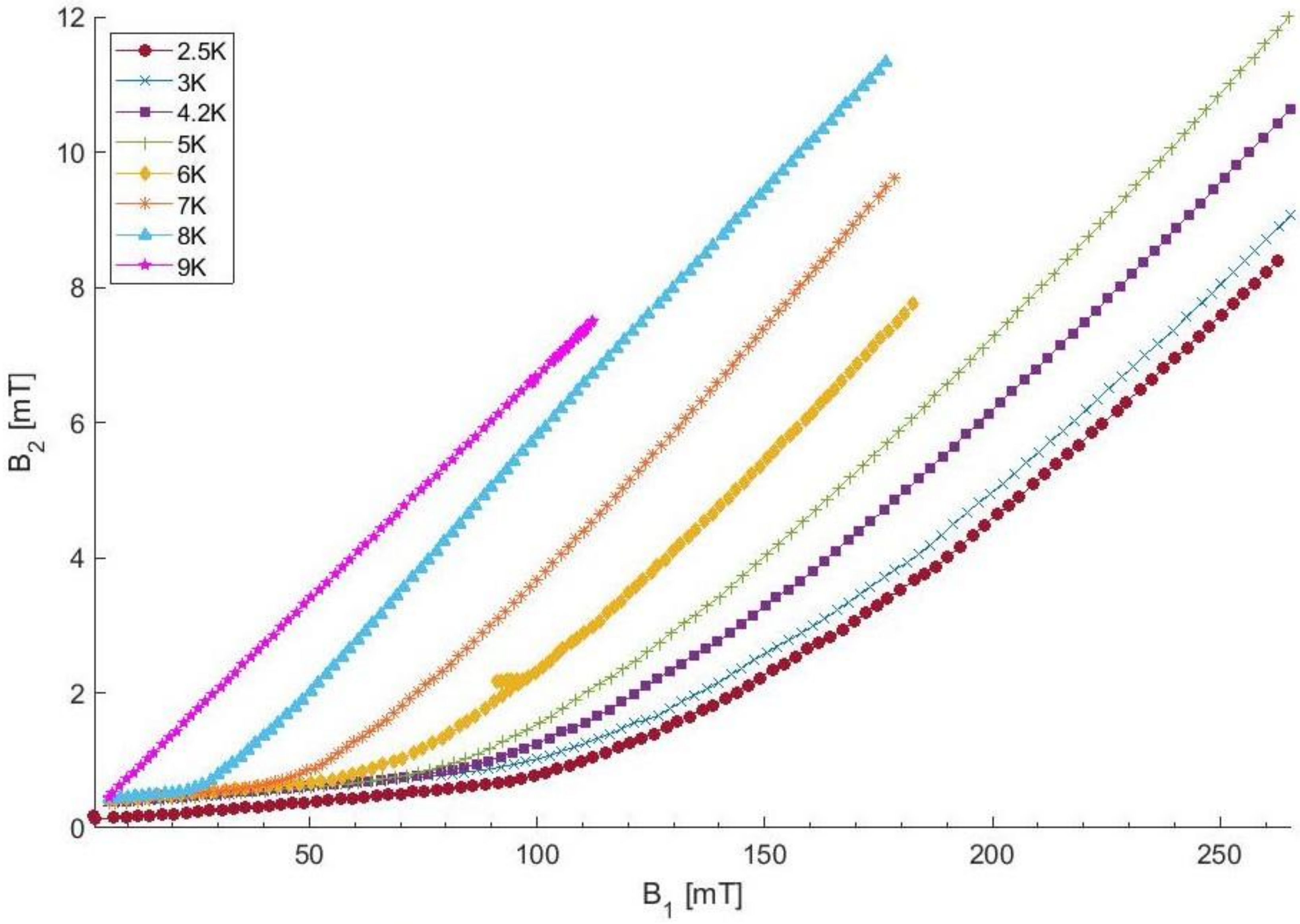

(Left) Raw data for 3.6 µm of Nb on a Cu disk with a diameter of 50 mm.

- Three Nb samples of varying thickness were deposited at STFC Daresbury Laboratory courtesy of Reza Valizadeh, with thickness' of 1.3, 3.6 and 5.1 µm to determine the effect of thickness on B_{fp}.
- The transition for Nb is much more gradual than compared to Pb.

Type II results - Nb

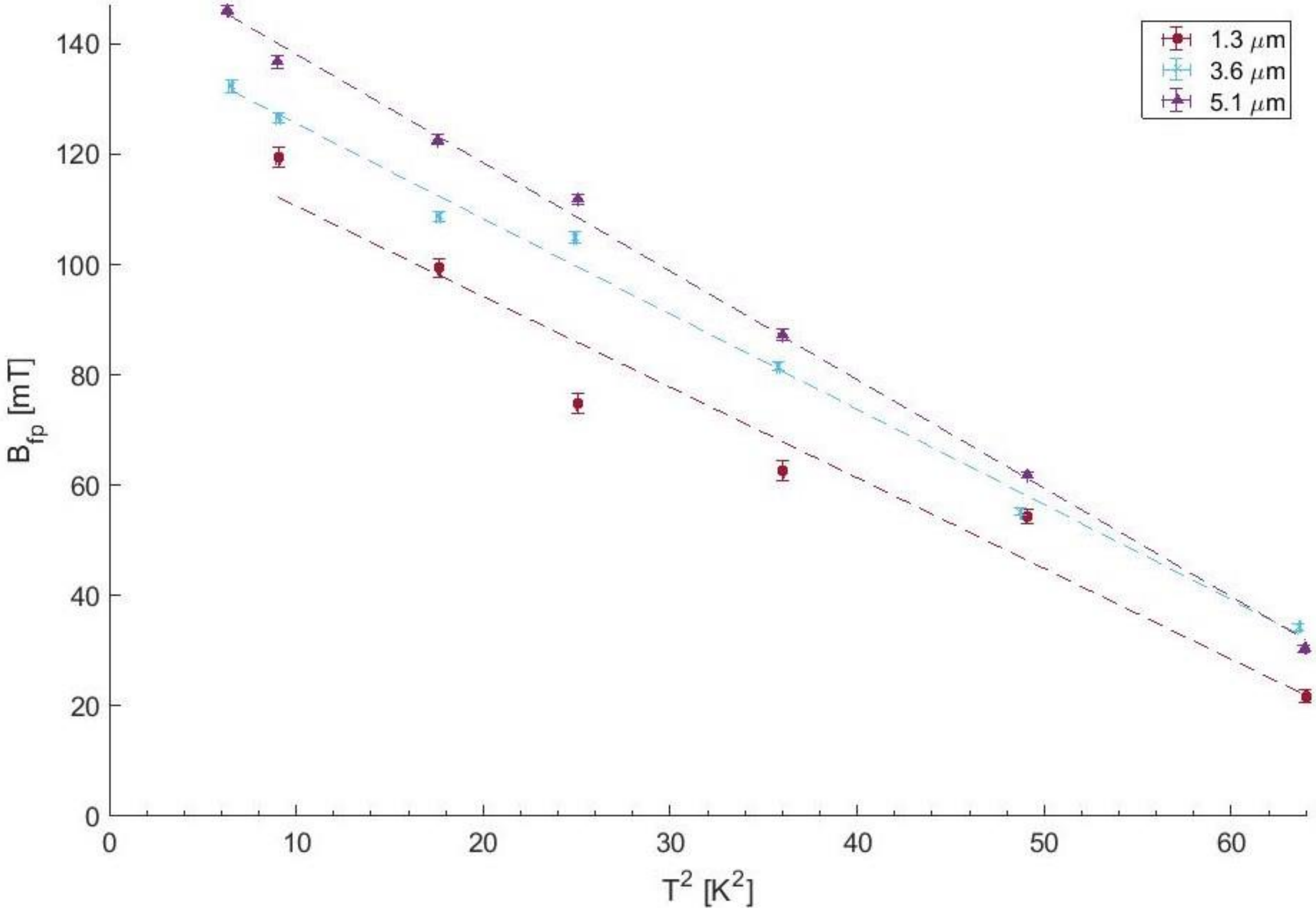

- The data is much noisier for the Nb samples.
- Thicker samples have an increased B_{fp}.
- More thickness' need to be tested to try and determine a relationship in B_{fp} and thickness.

ARIES WP15 – SRF thin film program

- The aim of the program was to develop superconducting cavities using thin film coatings:
  - Cu is cheaper than bulk Nb.
  - Improved thermal stability.
  - Insensitive to the earths magnetic field, so magnetic shielding not required.
  - Deposited Nb free from impurities unlike bulk Nb sheets.
- The surface quality of the substrate affects the growth of the Nb film.
- Cu substrates were polished using; Chemical polishing (SUBU) at either CERN or INFN LNL, electropolishing (EP), both EP and SUBU or Tumbling.
- Nb thin films were deposited on the surface of the substrates at INFN Legnaro, University of Siegen and STFC Daresbury laboratory.
- Superconducting properties of the samples were then tested using vibrating sample magnetometry (VSM) at the Institute of Electrical Engineering in Bratislava, and a new technique developed at STFC Daresbury.

The effect of polishing – ARIES samples

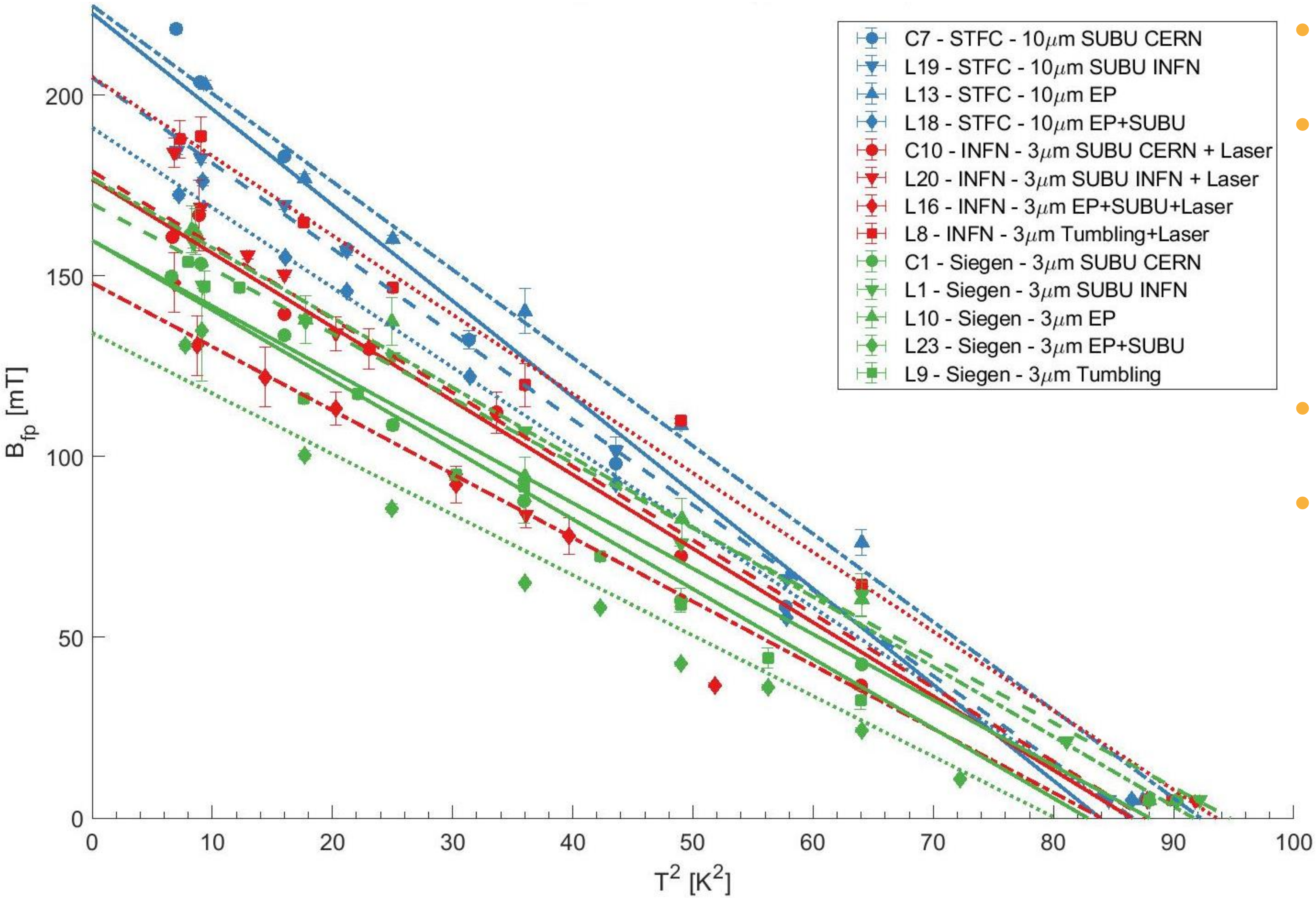

- 13 samples were tested using the field penetration method.
- All deposition run had a varying factor.
  - STFC samples were 10μm instead of 3μm.
  - INFN samples had been laser treated post deposition.
- STFC samples (due to a greater thickness) have a greater B_{fp}.
- Samples deposited at INFN LNL have the next best B_{fp} performance, followed by the samples deposited at University of Siegen.

The effect of polishing – Aries samples

STFC		Siegen		INFN (with laser polishing sample surface)		
Polishing method	**B_{fp}(0 K) [mT]**	**Polishing method**	**B_{fp}(0 K) [mT]**	**Polishing method**	**B_{fp}(0 K) [mT]**	
EP	224.7±8.5	EP	177.0±6.1			Largest B_{fp}(0 K)
				Tumbling	205.0±7.8	
SUBU CERN	222.6±0.9	SUBU INFN	169.9±5.1	SUBU INFN	178.9±2.2	
SUBU INFN	204.8±6.9	SUBU CERN	159.7±1.4	SUBU CERN	176.7±4.3	
		Tumbling	159.8±1.6			
EP + SUBU	191.0±4.3	EP + SUBU	134.2±1.1	EP + SUBU	148.0±3.7	Lowest B_{fp}(0 K)

Conclusion

- An idea for a field penetration measurements has been realised in the facility;
  - The facility has been designed, built, commissioned and is now in full time operation.
    - A cryogen free system has been designed, built and tested at Daresbury Laboratory
    - Applies a local DC field from one side to the other, T_{min} = 2.5 K, B_{max} ~ 612 mT at I = 8 A
    - Data acquisition is fully automated.
- The effect of sample geometry has been tested using a Pb sample.
- The effect of (Type II) sample thickness has been tested using Nb samples deposited.
- Multiple Nb samples deposited by ARIES WP15 partners with various substrate treatments have been tested:
  - Magnetic Field Penetration of Niobium Thin Films Produced by the Aries Collaboration (vrws.de)
- The ARIES thin film Nb samples have been laser treated and tested, with recent surface analysis measurements. Correlation between the magnetic field penetration method and surface analysis are ongoing.

- This work has led to my PhD thesis.

- Non-Nb films such as NbTiN and Nb_3Sn.
- Future plans for the facility within IFAST WP9:
  - SIS structures – Test thin films shielding substrate
  - Compare DC magnetometry with RF tests
  - Final stage – Implement the best films into cavity.

Acknowledgements

- CERN: A. Sublet
- IEE: E. Seiler, R. Ries
- INFN: C. Pira, E. Chyhyrynets
- RTU: A. Medvids, P. Onufrievs
- Siegen University: M. Vogel, S. Leith
- STFC/CI: O.B. Malyshev, R. Valizadeh, K. Dumbell, J.T.G. Wilson, J. Conlon, L. Smith, F. Lockwood Estrin, F. Walk, N. Pattalwar, S. Pattalwar, A. May
- Lancaster University/CI: G. Burt
- University of Victoria: T. Junginger

This research has been supported by European Commission's ARIES collaboration H2020 Research and Innovation Programme under Grant Agreement no. 730871.

Published papers

- Daniel A Turner et al, “No interface energy barrier and increased surface pinning in low temperature baked niobium”, Scientific Reports 12 (1), 1-9 (2022).

Proceedings

- Daniel A Turner et al, “Characterization of flat multilayer thin film superconductors”, in proc SRF 2019
- Daniel A Turner et al, “Magnetic field penetration of niobium thin films produced by the aries collaboration”, in proc SRF 2021
- Oleg B. Malyshev, Daniel A Turner et al, “Main Highlights of ARIES WP15 Collaboration”, in proc SRF 2021
- R Valizadeh, AN Hannah, S Aliasghari, OB Malyshev, GBG Stenning, Daniel A Turner, K Dawson, VR Dahnak “PVD Depostion of Nb3Sn thin film on copper substrate from an alloy Nb3Sn target”, Proc. IPAC'19, 2818-2821

Submitted papers

- Daniel A Turner, Oleg B Malyshev, Graeme Burt, Tobias Junginger, Reza Valizadeh, Lewis Gurran, “A facility for the characterisation of planar multilayer structures with preliminary Niobium results” – Submitted to Superconducting science and technology (2022)

Soon to be submitted papers

- Daniel A Turner et al, “The effect of laser treatment on sputtered niobium thin films on copper substrates using a magnetic field penetration facility” – Submission by the end of this month

Thank you for your attention

Finding B_{fp}

Normalisation method

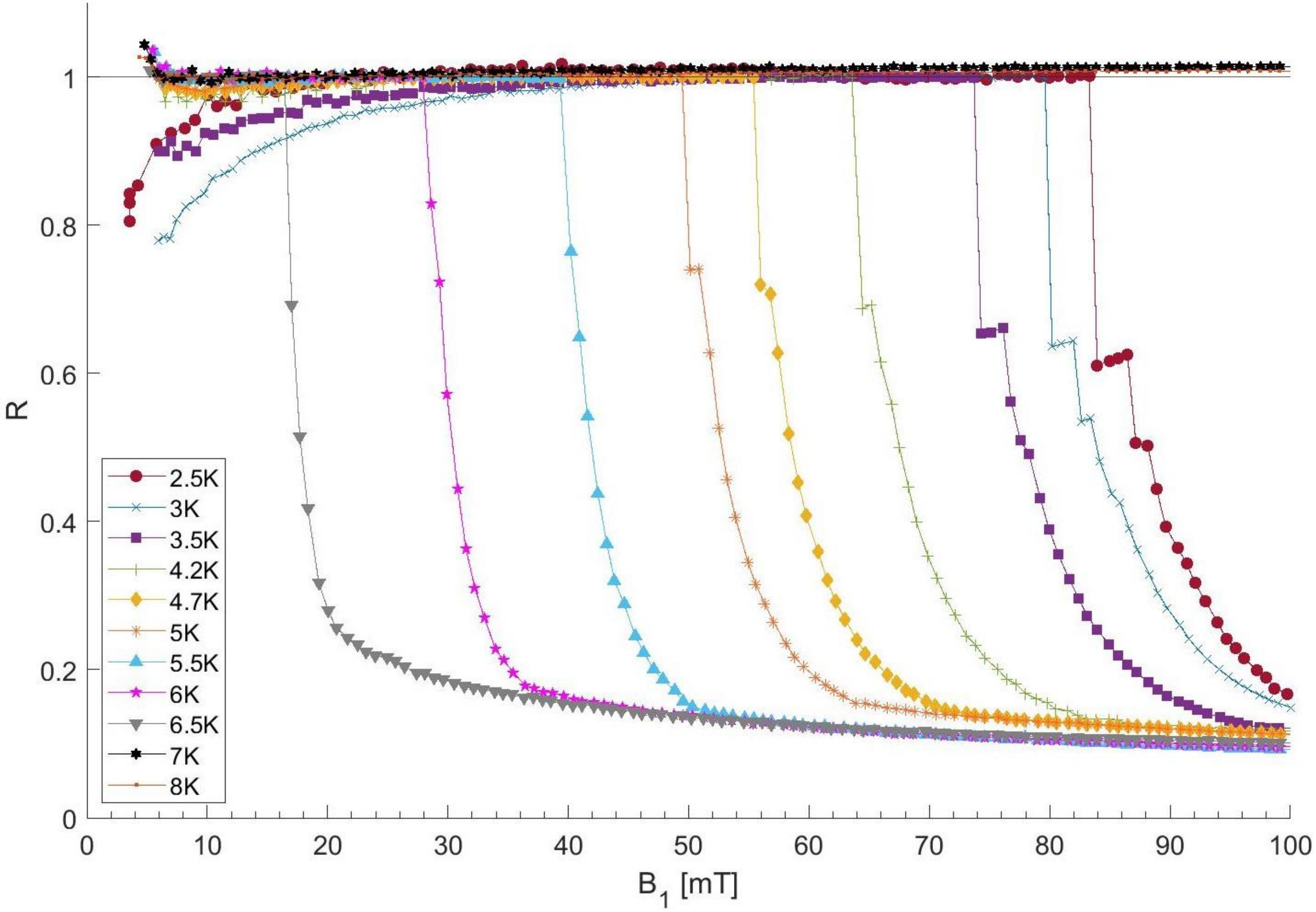

Ratio method:

- An infinitely large sample can be described as no B leaking around the sample:

$$R = 1 - \frac{B_2}{B_1 K_1}$$

- However, as the samples are a finite size B_1K_2 must be taken into account:

$$R = 1 - \frac{B_2 - B_1 K_2}{B_1 K_1}$$

- Which can be simplified to:

$$R = 1 + \frac{K_2}{K_1} - \frac{B_2}{B_1 K_1}$$

- However, this method is only reliable for samples with a sharp transition for B_{fp}

Data for the Pb sample

A comparison for the leakage factor and extrapolated values for B_{fp} and T_c using the Normalisation method (Method 1) and the second derivative method (method 2)

Run	Length (x axis) [mm]	Width (z axis) [mm]	$K_2[10^{-3}]$	$B_{fp}(0K)$ [mT]	T_c[K]	$B_{fp}(0K)$ [mT]	T_c[K]
				Method 1		Method 2	
Original	50	50	7.6 ± 0.9	96.0 ± 0.3	7.10 ± 0.01	96.7 ± 0.3	7.16 ± 0.01
1st cut	50	45	8.3 ± 1.4	94.9 ± 0.3	7.15 ± 0.01	96.0 ± 0.3	7.19 ± 0.01
2nd cut	50	40	7.5 ± 0.8	95.7 ± 0.3	7.21 ± 0.01	96.6 ± 0.3	7.23 ± 0.01
Rotation	40	50	11.0 ± 1.0	98.9 ± 0.4	7.14 ± 0.02	101.8 ± 0.6	7.12 ± 0.04
3rd cut	50 mm Disk		11.0 ± 2.0	95.4 ± 0.3	7.15 ± 0.01	96.3 ± 0.3	7.17 ± 0.01
4th cut	40	30	17.5 ± 1.3	89.3 ± 0.4	7.12 ± 0.02	89.9 ± 0.4	7.16 ± 0.02
5th cut	30	30	24.1 ± 1.2	76.9 ± 0.3	7.08 ± 0.02	84.4 ± 1.1	7.08 ± 0.09
6th cut	20	20	47.3 ± 4.0	60.8 ± 0.3	6.98 ± 0.02	57.5 ± 1.3	7.28 ± 0.16

B_{fp}(0K) as a function of sample length

Pb - B_{fp} taken using the second derivative method